

# TEMPERED FRACTIONAL BROWNIAN MOTION: WAVELET ESTIMATION AND MODELING OF TURBULENCE IN GEOPHYSICAL FLOWS

B. C. Boniece<sup>1</sup>, F. Sabzikar<sup>2</sup>, G. Didier<sup>1</sup>

<sup>1</sup> Mathematics Department, Tulane University, New Orleans, USA.

<sup>2</sup> Statistics Department, Iowa State University, USA.

## ABSTRACT

Fractional Brownian motion (fBm) is a Gaussian, stationary-increment process whose self-similarity property is governed by the so-named Hurst parameter  $H \in (0, 1)$ . fBm is one of the most widely used models of scale invariance, and its instance  $H = 1/3$  corresponds to the classical Kolmogorov spectrum for the inertial range of turbulence. Tempered fractional Brownian motion (tfBm) was recently introduced as a new canonical model that displays the so-named Davenport spectrum, a model that also accounts for the low frequency behavior of turbulence. The autocorrelation of its increments displays semi-long range dependence, i.e., hyperbolic decay over moderate scales and quasi-exponential decay over large scales. The latter property has now been observed in many phenomena, from wind speed to geophysics to finance. This paper introduces a wavelet framework to construct the first estimation method for tfBm. The properties of the wavelet coefficients and spectrum of tfBm are studied, and the estimator's performance is assessed by means of Monte Carlo experiments. We also use tfBm to model geophysical flow data in the wavelet domain and show that tfBm provides a closer fit than fBm.

**Index Terms**— Wavelets, semi-long range dependence, tempered fractional models, geophysical turbulence

## 1. INTRODUCTION

**Turbulence modeling and fractional Brownian motion.** Classical models of turbulence describe how kinetic energy at the largest length scales is progressively transferred down to smaller scales. In the complete Kolmogorov spectral model for turbulence [1–3], large eddies are produced in the low frequency range of scales, whereas in the inertial range (moderate frequencies), larger eddies are continuously broken down into smaller eddies, until they eventually dissipate (high frequencies). In particular, the energy spectrum  $f$  in the inertial range decreases according to a power law  $f(x) \propto |x|^{-5/3}$ .

In their landmark paper [4], Mandelbrot and Van Ness revisited Kolmogorov's model by proposing fractional Brownian motion (fBm) as a framework for the analysis of *scale invariant* (non-Markovian) phenomena. A system is called scale invariant if its dynamics are driven by a continuum of time scales instead of a few characteristic scales. fBm is defined as a Gaussian, self-similar stochastic process with stationary increments [5] and it is among the most widely used scale invariance models. Its stochastic behavior is essentially characterized by the so-named Hurst parameter  $H \in (0, 1)$ , where the instance  $H = 1/3$  corresponds to the Kolmogorov spectrum.

**Tempered fractional models and applications.** In [6], a modification of the Kolmogorov spectrum, nowadays called the Davenport spectrum, is proposed that accounts for the low frequency behavior of turbulence (not included in Kolmogorov's model for the inertial range). Such framework has been successfully used in wind speed modeling [7–9]. Accordingly, [10–12] introduced a new canonical model, called *tempered fractional Brownian motion* (tfBm), which displays the Davenport spectrum. TfBm exhibits *semi-long range dependence*, i.e., the correlation between increments decays approximately like a power law over fine/moderate scales (fractional behavior or scale invariant), but exponentially over large scales [13]. This is a consequence of an extra (tempering) parameter  $\lambda > 0$  that controls the deviation from a fBm spectrum at low frequencies. TfBm and, more generally, tempered fractional processes (ART-FIMA, tempered diffusion, tempered stable motions, tempered Lévy flights) have recently been studied and used in a wide range of modern applications such as in the modeling of transient anomalous diffusion [14], geophysical flows [15] and finance [16].

**Scale-free dynamics and wavelets.** The wavelet transform is a powerful tool for the analysis of scale invariant phenomena. Given an observed fractional time series  $X$ , estimation of the parameter  $H$  can be conducted by a log-regression procedure that draws upon the scaling property of the sample wavelet variance [17–19], i.e.,

$$\frac{1}{n_j} \sum_{k=1}^{n_j} d_X^2(j, k) \simeq C 2^{j(2H+1)}, \quad (1)$$

where  $C > 0$  is a constant and  $d_X(j, k)$ ,  $k = 1, \dots, n_j$ , is the wavelet transform at scale  $2^j$  and shift  $k$ . Wavelet-based statistical inference has well-documented benefits, such as: (i) computational efficiency [19]; (ii) robustness with respect to contamination by trends [20]; (iii) modeling of stationary or stationary increment processes of any order in the same framework; (iv) quasi-decorrelation of several families of stochastic processes [21, 22], which often leads to Gaussian confidence intervals. However, little work has been done, in general, on statistical methodology for tempered fractional processes. In [15], turbulence data is modeled in the Fourier domain within an ARTFIMA framework. In [23], a wavelet log-regression method is constructed for a subclass of tempered fractional processes assuming the tempering parameter  $\lambda$  is known. In sharp contrast to the situation for fBm, to the best of our knowledge no estimator has been proposed for tfBm. Moreover, for any tempered process, the literature lacks a wavelet-based method that tackles jointly the Hurst parameter  $H$  and the tempering parameter  $\lambda$ .

**Goals, contributions and outline.** In this paper, we construct the first (wavelet-based) estimator for tfBm. We establish the wavelet analysis of tfBm and for the first time describe the phenomenon

---

G.D. was partially supported by the ARO grant W911NF-14-1-0475.

of semi-long range dependence in the wavelet domain. The finite sample and asymptotic performance of the estimator is assessed and compared to Fourier-domain (Whittle) estimation. This includes the characterization of the estimable range of  $\lambda$  for given sample sizes. We also use tfBm to model geophysical flow data from the Red Cedar River in Michigan and compare the fit with that obtained from fBm. For space reasons, all theoretical results will be detailed in a forthcoming paper [32].

## 2. TEMPERED FRACTIONAL BROWNIAN MOTION

**Definition.** For  $\lambda, H > 0$ , TfBm is the stochastic process defined by the harmonizable representation

$$B_{H,\lambda}(t) = \frac{\Gamma(H + \frac{1}{2})}{\sqrt{2\pi}} \int_{\mathbb{R}} \frac{e^{ixt} - 1}{(\lambda + ix)^{H + \frac{1}{2}}} \tilde{B}(dx), \quad t \in \mathbb{R}, \quad (2)$$

where  $\tilde{B}(dx)$  is a complex-valued Gaussian random measure such that  $\tilde{B}(-dx) = \overline{\tilde{B}(dx)}$  and  $\mathbb{E}|\tilde{B}(dx)|^2 = \sigma^2 dx$ .

Expression (2) implies that tfBm is Gaussian and has stationary increments. Moreover, starting from its corresponding moving average representation [10], it can be shown that its covariance function  $\gamma(s, t) = \text{Cov}(B_{H,\lambda}(s), B_{H,\lambda}(t))$  can be expressed as

$$\gamma(s, t) = \frac{\sigma^2}{2} \left\{ C_t^2 |t|^{2H} + C_s^2 |s|^{2H} - C_{t-s}^2 |t-s|^{2H} \right\}$$

for  $s, t \in \mathbb{R}$ , where  $C_t^2 := \frac{2\Gamma(2H)}{(2\lambda|t|)^{2H}} - \frac{2\Gamma(H + \frac{1}{2})}{\sqrt{\pi}} \frac{K_H(\lambda|t|)}{(2\lambda|t|)^H}$ ,  $t \neq 0$ ,  $K_\nu(z)$  is the modified Bessel function of the second kind, and  $C_0^2 = 0$ . When  $0 < H < 1$ , and  $\lambda = 0$ , the representation (2) reduces to a fBm with Hurst parameter  $H$ . Unlike fBm, when  $\lambda > 0$ , tfBm is not a self-similar process, but instead satisfies the scaling relation

$$\{B_{H,\lambda}(ct)\}_{t \in \mathbb{R}} \stackrel{\mathcal{L}}{=} \left\{ c^H B_{H,c\lambda}(t) \right\}_{t \in \mathbb{R}},$$

where  $\stackrel{\mathcal{L}}{=}$  denotes equality of finite-dimensional distributions. Notably, even though nonstationary, tfBm converges almost surely to a stationary process as  $t \rightarrow \infty$ . This property of tfBm makes it suitable for modeling data that looks stationary or converges to stationarity. The increment process of tfBm, namely,  $\{X(t)\}_{t \in \mathbb{Z}} := \{B_{H,\lambda}(t+1) - B_{H,\lambda}(t)\}_{t \in \mathbb{Z}}$ , is called *tempered fractional Gaussian noise* (tfGn). Its covariance function  $\gamma_X(h) = \mathbb{E}X(t)X(t+h)$ ,  $h \in \mathbb{Z}$ , has decay

$$\gamma_X(h) \sim \frac{\sigma^2 \Gamma(H + \frac{1}{2})(e^{-\lambda} + e^\lambda - 2)}{(2\lambda)^{H+1/2}} \frac{h^{H-1/2}}{e^{\lambda h}}, \quad h \rightarrow \infty,$$

i.e., its decay is hyperbolic for small lags values  $h$  but quasi-exponential for large  $h$  when  $\lambda > 0$  is small (semi-long range dependence).

## 3. WAVELET-BASED ESTIMATION

Following seminal work on estimation methodology for fractional stochastic processes (e.g., [17, 18, 24, 25] to cite just a few references), we construct a wavelet estimation framework for tfBm. With classical fBm and related processes, only coarse scale information is generally of interest, which is given by the Hurst parameter  $H$ . By contrast, with tfBm, fine/moderate scale information is also relevant and is provided by  $H$ , whereas on coarse scales it is given by both  $H$

and  $\lambda$ . This calls for parametric estimation. In view of the fact that only finitely many observations are available in practice, for greater accuracy we construct the wavelet analysis directly in discrete time, in lieu of its more elegant continuous time approximation.

**Discrete wavelet transform (DWT) in discrete time.** A mother wavelet  $\psi \in L^2(\mathbb{R})$  is a function satisfying  $\int_{\mathbb{R}} t^p \psi(t) dt = 0$  for  $p = 0, 1, \dots, N_\psi - 1$  and  $\int_{\mathbb{R}} t^{N_\psi} \psi(t) dt \neq 0$ , where  $N_\psi$  is called the number of vanishing moments. Considering a Daubechies multiresolution analysis (MRA) of  $L^2(\mathbb{R})$  [19], the dilations and translations  $\{\psi_{j,k}(t)\}_{j,k \in \mathbb{Z}}$ ,  $\psi_{j,k}(t) := 2^{-j/2} \psi(2^{-j}t - k)$ , of the wavelet function form an orthonormal basis of  $L^2(\mathbb{R})$ .

Given a time series  $\{B_{H,\lambda}(k)\}_{k \in \mathbb{Z}}$ , we initialize Mallat's algorithm with the sequence  $a_{0,k} := B_{H,\lambda}(k)$ ,  $k \in \mathbb{Z}$ , also called the approximation coefficients at scale  $2^0 = 1$ . At coarser scales  $2^j$ , the algorithm is characterized by the iterative procedure

$$a_{j+1,k} = \sum_{k' \in \mathbb{Z}} u_{k'-2k} a_{j,k'}, \quad d_{j+1,k} = \sum_{k' \in \mathbb{Z}} v_{k'-2k} a_{j,k'},$$

$j \in \mathbb{N}$ ,  $k \in \mathbb{Z}$ , where the filter sequences  $\{u_k := 2^{-1/2} \int_{\mathbb{R}} \phi(t/2) \phi(t-k) dt\}_{k \in \mathbb{Z}}$ ,  $\{v_k := 2^{-1/2} \int_{\mathbb{R}} \psi(t/2) \phi(t-k) dt\}_{k \in \mathbb{Z}}$  are called low- and high-pass MRA filters, respectively. Due to the compactness of the supports of  $\psi$  and the associated scaling function  $\phi$ , only a finite number of filter terms is nonzero, which is computationally convenient [26]. The wavelet coefficients  $d(j, k)$  can then be expressed as

$$d(j, k) = \sum_{l \in \mathbb{Z}} B_{H,\lambda}(l) h_{j,2^j k - l}, \quad (3)$$

where  $h_{j,l} := 2^{-j/2} \int_{\mathbb{R}} \phi(t+l) \psi(2^{-j}t) dt$ . From the above assumptions, it can be shown that, for fixed scales  $j$  and  $j'$  and some constant  $C_{N_\psi}$ ,

$$|\text{Cov}(d(j, k), d(j', k'))| \leq C_{N_\psi} 2^{(j+j')/2} \frac{|2^j k - 2^{j'} k'|^{H-\frac{1}{2}}}{e^{\lambda |2^j k - 2^{j'} k'|}}, \quad (4)$$

i.e., semi-long range dependence carries over to the wavelet domain.

**Wavelet analysis and semi-long range dependence.** Let  $\mathcal{H}_j(x) = \sum_{l \in \mathbb{Z}} h_{j,l} e^{ixl} \in \mathbb{C}$  be the discrete Fourier transform of the sequence  $\{h_{j,l}\}_{l \in \mathbb{Z}}$  appearing in (3). The harmonizable representation of tfBm (2), expression (3) and the periodicity of  $\mathcal{H}_j$  imply that

$$\mathbb{E}d^2(j, k) = \frac{\sigma^2}{2\pi} \int_{-\pi}^{\pi} \sum_{l \in \mathbb{Z}} \frac{\Gamma^2(H + \frac{1}{2}) |\mathcal{H}_j(x)|^2}{|\lambda^2 + (x + 2\pi l)^2|^{H+\frac{1}{2}}} dx, \quad (5)$$

regardless of  $k \in \mathbb{Z}$ . The wavelet spectrum of tfBm is depicted in Figure 1. The semi-long range dependence phenomenon manifests itself as follows. For small  $\lambda > 0$ , the wavelet spectrum of  $B_{H,\lambda}(t)$  mimics that of fBm for moderate scales  $2^j$ , namely, it is approximately linear with slope  $2H + 1$ . However,

$$\lim_{j \rightarrow \infty} \mathbb{E}d^2(j, 0) = \sum_{l \in \mathbb{Z}} \frac{\sigma^2 \Gamma^2(H + \frac{1}{2})}{|\lambda^2 + (2\pi l)^2|^{H+\frac{1}{2}}}, \quad (6)$$

i.e., it tends to a constant at large octaves, where the transition from linearity to constancy is controlled by the tempering parameter  $\lambda > 0$ .

**Parameter estimation.** An  $M$ -estimator [27] can be constructed based on the (whole) wavelet spectrum of tfBm. For a number  $n$  of observations of a tfBm, define the sample wavelet variance  $W(j) = \frac{1}{n_j} \sum_{k=1}^{n_j} d^2(j, k)$ ,  $n_j = \frac{n}{2^j}$ ,  $j = j_1, \dots, j_2$ , for some octave range

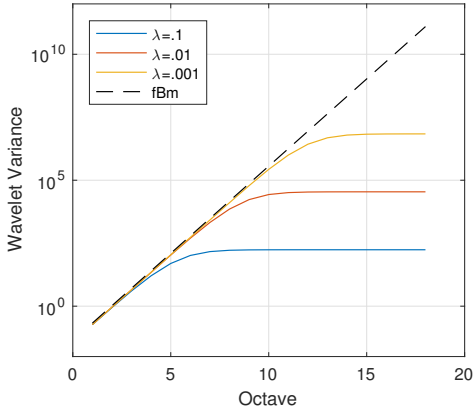


**Fig. 1. Semi-long range dependence in the wavelet spectrum.** The smaller the value of  $\lambda > 0$ , the wider the range of octaves  $j$  over which the wavelet spectrum of tfBm resembles that of fBm.

$1 \leq j_1 \leq j_2 \leq \lfloor \log_2(n) \rfloor$ , where the sample wavelet coefficients  $d(j, k)$  are computed by means of the expression (3). Let  $\theta = (H, \lambda, \sigma^2)$  be the parameter vector. We define a wavelet-based estimator by means of a weighted nonlinear log-regression

$$\hat{\theta} := \arg \min_{\theta} \sum_{j=j_1}^{j_2} w_j (\log_2 W(j) - \eta_j(\theta))^2, \quad (7)$$

where the octaves  $j_1$  and  $j_2$  are chosen so as to capture both the fine/moderate-scale behavior and the limiting behavior (6). In (7),  $\eta_j$  is an appropriate choice of log-wavelet spectrum function. There are two effects to consider when picking  $\eta_j$  and  $w_j$ . First, estimation based on minimizing the distance between  $W(j)$  and  $\log_2 \mathbb{E}d^2(j, 0)$  is biased due to the fact that  $\mathbb{E} \log_2 d^2(j, 0) \neq \log_2 \mathbb{E}d^2(j, 0)$ . Second, the variance of the sample wavelet variance  $W(j)$  changes across scales. In view of the near decorrelation property (4), we propose using bias-corrected and rescaled wavelet spectrum expressions in (7) by applying standard approximations to  $\mathbb{E} \log W(j)$  and  $\text{Var} \log W(j)$  [18, 28]. More precisely, on one hand we set the wavelet spectrum functions to

$$\eta_j(\theta) = \log_2 \mathbb{E}d^2(j, 0) + B(j), \quad j = j_1, \dots, j_2,$$

where  $B(j) = \frac{\Psi(n_j/2)}{\log 2} - \log_2 \left( \frac{n_j}{2} \right)$  for  $\Psi(z) = \Gamma'(z)/\Gamma(z)$ ,  $z > 0$ . On the other hand, we choose the weights  $w_j = 1/2^{(j-1)/2}$ ,  $j = j_1, \dots, j_2$ .

**Estimation implementation and performance.** Computational experiments show that assuming  $\sigma^2$  is known does not qualitatively change the results, so for convenience we set it to 1. The performance of the estimator  $(\hat{H}, \hat{\lambda})$  is assessed by means of Monte Carlo experiments performed over 5000 independent realizations of tfBm. Even though tfBm is well-defined for  $H \geq 1$ , for physical reasons we focus on the range  $H \in (0, 1)$ . The chosen range of parameter values is  $(H, \lambda) \in \{0.15, 0.35, 0.65, 0.85\} \times \{0.001, 0.01, 0.1, 1\}$ . The sample size values  $n = 2^{12}$  and  $2^{20}$  were picked as to reflect a realistic time series length and the asymptotic regime, respectively. The generation of tfBm is done based on circulant matrix embedding for tfGn [29, 30]. To implement the wavelet variances appearing in the objective function on the right-hand side of (7),

	wavelet, $n = 2^{12}$			
	$H = 0.15$	$H = 0.35$	$H = 0.65$	$H = 0.85$
$\lambda = 0.001$	(.1523, .0031) (.0041, .0048)	(.3564, .0025) (.0124, .0037)	(.6584, .0020) (.0206, .0030)	(.8576, .0017) (.0199, .0025)
$\lambda = 0.01$	(.1503, .0102) (.0034, .0073)	(.3499, .0101) (.0110, .0057)	(.6495, .0101) (.0231, .0046)	(.8494, .0101) (.0244, .0039)
$\lambda = 0.1$	(.1504, .1003) (.0031, .0170)	(.3501, .1002) (.0070, .0128)	(.6500, .1003) (.0184, .0111)	(.8504, .1002) (.0349, .0129)
$\lambda = 1$	(.1504, 1.016) (.0046, .1648)	(.3502, 1.004) (.0090, .0715)	(.6502, 1.001) (.0161, .0417)	(.8505, 1.000) (.0220, .0318)

	wavelet, $n = 2^{20}$			
	$H = 0.15$	$H = 0.35$	$H = 0.65$	$H = 0.85$
$\lambda = 0.001$	(.1504, .0010) (.0003, .0001)	(.3502, .0010) (.0008, .0001)	(.6501, .0010) (.0013, .0001)	(.8501, .0010) (.0013, .0001)
$\lambda = 0.01$	(.1504, .0100) (.0002, .0002)	(.3503, .0100) (.0006, .0002)	(.6500, .0100) (.0013, .0002)	(.8500, .0100) (.0014, .0001)
$\lambda = 0.1$	(.1504, .1000) (.0002, .0009)	(.3503, .1000) (.0004, .0006)	(.6501, .1000) (.0011, .0006)	(.8501, .1000) (.0019, .0007)
$\lambda = 1$	(.1504, .9995) (.0002, .0082)	(.3504, .9998) (.0005, .0039)	(.6501, 1.000) (.0009, .0023)	(.8500, 1.000) (.0013, .0017)

	Whittle, $n = 2^{12}$			
	$H = 0.15$	$H = 0.35$	$H = 0.65$	$H = 0.85$
$\lambda = 0.001$	(.1505, .0016) (.0028, .0019)	(.3508, .0018) (.0056, .0016)	(.6507, .0018) (.0086, .0012)	(.8509, .0018) (.0102, .0010)
$\lambda = 0.01$	(.1504, .0065) (.0029, .0041)	(.3501, .0083) (.0055, .0031)	(.6494, .0091) (.0103, .0023)	(.8492, .0094) (.0107, .0020)
$\lambda = 0.1$	(.1504, .0658) (.0028, .0306)	(.3499, .0827) (.0057, .0187)	(.6486, .0905) (.0102, .0120)	(.8468, .0924) (.0129, .0098)
$\lambda = 1$	(.1573, .6100) (.0060, .3070)	(.3628, .7989) (.0127, .1906)	(.6664, .8961) (.0189, .1093)	(.8680, .9252) (.0227, .0833)

**Table 1. Estimation of  $H$  and  $\lambda$ .** Each of the entries in the above tables corresponds to the Monte-Carlo averages (top row of each cell) and standard deviations (bottom row of each cell), based on 5000 independent realizations per  $(H, \lambda)$  pair.

we truncate the summation in (5) at  $|l| \leq 10$ . Noting that for  $K$  sufficiently large we have  $\sum_{|l| > K} |\lambda^2 + (x + 2\pi l)^2|^{-(H+\frac{1}{2})} \approx \sum_{|l| > K} |\lambda^2 + (2\pi l)^2|^{-(H+\frac{1}{2})}$  for all  $x \in [-\pi, \pi]$ , we approximate the remaining terms in the summation using the integral  $2 \int_{10}^{\infty} \Gamma^2(H + \frac{1}{2}) (2\pi)^{-1} |\lambda^2 + (2\pi l)^2|^{-(H+\frac{1}{2})} dl$ . Minimization of the objective function (7) was carried out by means of the Matlab routine `fmincon` with constraints  $0 < H < 1$ ,  $0 < \lambda < 5$  and initial values  $(\hat{H}_{\text{init}}, \hat{\lambda}_{\text{init}}) = (1/2, 0.03)$ . In all cases, we set  $j_1 = 1$ . The value  $j_2$  plays an important role in determining what range of  $\lambda$  can be estimated; larger values of  $j_2$  correspond to improved estimation of increasingly smaller  $\lambda > 0$ . However, inclusion of additional scales in the  $M$ -estimator (7) also adds to the computational cost of the optimization. Thus, for the large sample size  $n = 2^{20}$  we set  $j_2 = 12$ , and for the moderate sample size  $n = 2^{12}$ , we set  $j_2 = j_{\text{max}}$ , where  $j_{\text{max}}$  is the largest available octave in the sample. Similarly to classical fBm (c.f. [31]), numerical results indicate that  $N_\psi = 2$  is optimal for  $H > 1/2$  when  $\lambda$  is small due to the semi-long range dependence phenomenon. For other parameter values, other choices for  $N_\psi$  performed similarly. So, we set  $N_\psi = 2$  for this study, giving  $j_{\text{max}} = 10$  for  $n = 2^{12}$ .

Figure 2 shows the asymptotic normality of the estimators  $\hat{H}$  and  $\hat{\lambda}$ . As the sample size increases, the qq-plots reflect convergence to normal distributions. In fact, it can be shown that, under mild as-

sumptions, the estimator  $(\hat{H}, \hat{\lambda})$  is asymptotically normal (hence, consistent), i.e.,  $\sqrt{n}((\hat{H}, \hat{\lambda}) - (H, \lambda)) \xrightarrow{d} N(0, \Sigma)$ ,  $n \rightarrow \infty$ , for some symmetric positive semidefinite matrix  $\Sigma$  depending on the parameters. This results, in part, from the summability in  $k, k'$  of the wavelet covariance structure (see (4)). The finite sample performance results are shown in Table 1. For  $\lambda \geq 0.01$ , the wavelet estimator displays very small biases and good MSE performance in the estimation of  $(H, \lambda)$  for  $n = 2^{12}$ , and the biases tend to disappear for the very large sample size  $2^{20}$  for any value of  $\lambda$  or  $H$ . Interestingly, together Figure 1 and Table 1 visually and computationally indicate that the value .001 is a lower bound on the estimable  $\lambda$  parameter range at  $n = 2^{12}$  (and  $j_2 = 10$ ), since tfBm with  $\lambda = .001$  is almost indistinguishable from fBm at this sample size. Unreported results indicate that, on the other side, an upper bound on estimable values of  $\lambda$  is 3.

Since no other estimator is available for tfBm, to gauge the comparative performance of the wavelet estimator we further implemented Whittle estimation (for tfGn). The latter requires minimization of a Fourier domain objective function involving the spectral density of the process [33]. For the sake of comparison, we also truncate the Whittle objective function at  $|l| \leq 10$  terms, and approximate the remaining terms using the same integral as in the wavelet-based method. The Whittle estimator is significantly faster than the wavelet estimator, clocking 0.7 seconds per run, compared to 3.9 seconds of the latter. Statistically, the Whittle and wavelet method perform very similarly in the estimation of the parameter  $H$ . However, as compared to the wavelet method, the Whittle seems to consistently underestimate  $\lambda \geq 0.01$  especially for smaller values of  $H$ . It is an open question whether Whittle-type estimation can be improved – perhaps at a greater computational cost –, but this study serves to illustrate the general difficulty in estimating the parameter  $\lambda$ .

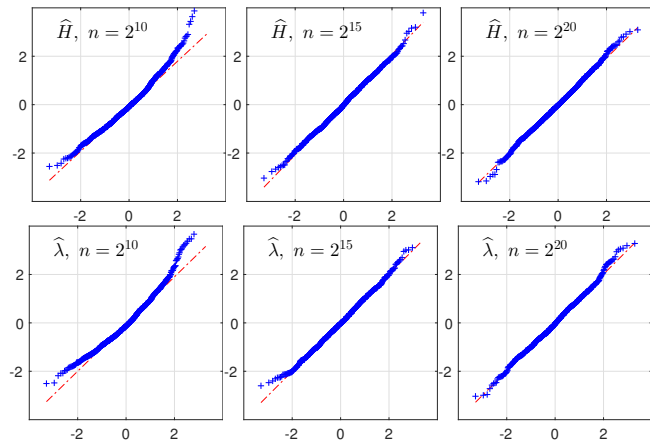


**Fig. 2. Asymptotic normality of  $(\hat{H}, \hat{\lambda})$ .** For fixed true parameter values  $(H, \lambda) = (0.75, 0.1)$ , the qq-plots show progress toward normality for sample sizes  $n = 2^{10}, 2^{15}, 2^{20}$  (left to right column, respectively).

#### 4. DATA MODELING

**Geophysical flow data.** As an application, we conduct wavelet domain analysis and modeling of velocity data associated with turbulent supercritical flow in the Red Cedar River, a fourth-order stream in Michigan (Coordinates: 42.72908N, 84.48228W). The data was

kindly provided by Prof. Mantha S. Phanikumar, from Michigan State University. This data set contains flow features over a range of spatial and temporal scales associated with turbulent flows in the natural environment and is believed to be appropriate for the analysis of energy spectra. The measurements ( $n = 46080$  points) were made at a sampling rate of 50 Hz using a 16 MHz Sontek Micro-ADV (Acoustic Doppler Velocimeter) on May 26, 2014. The same data set is modeled in [15] in the Fourier domain.

Figure 3 depicts the wavelet analysis of the Red Cedar River. The sample spectrum is close to that of a tfBm, and significantly deviates from that of a fBm. All three parameters were fitted, and the estimated values  $(\hat{H}, \hat{\lambda})$  are well within the range studied in Table 1. Moreover,  $\hat{H}$  is strikingly close to the theoretical value  $H = 1/3$  from Kolmogorov’s model for the inertial range (note that, in [15],  $H$  was set to  $1/3$  and only the tempering parameter  $\lambda$  was estimated).

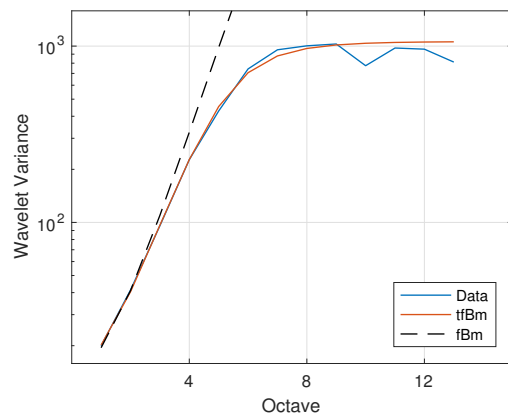


**Fig. 3. Sample wavelet spectrum for the Red Cedar River data.** As evidenced by the sample wavelet spectrum, tfBm provides a close fit for turbulent flow data. The wavelet-based estimates are  $\hat{H} = 0.329$ ,  $\hat{\lambda} = 0.121$ ,  $\hat{\sigma}^2 = 24.825$ . Note that  $\hat{H} \approx \frac{1}{3}$ , which is consistent with Kolmogorov scaling in the inertial range.

#### 5. CONCLUSION AND PERSPECTIVES

Tempered fractional Brownian (tfBm) motion is a recently introduced canonical model that displays the so-named Davenport spectrum. For tfBm, in addition to the Hurst parameter, a tuning parameter  $\lambda$  is used that controls the range of the inertial spectrum. In this paper, we construct for the first time the wavelet analysis of tfBm and propose a new nonlinear log-regression wavelet estimator. The estimator is consistent and asymptotically normal. Monte Carlo studies show that it has very good finite sample performance as compared to Fourier-domain estimation at an acceptable computational cost. Wavelet analysis of turbulent flow data collected from the Red Cedar River in Michigan shows that the tfBm spectrum is a good approximation, and the estimated parameter values are rather close to theoretical predictions stemming from Kolmogorov’s model. MATLAB routines will be made available at the time of publication. Future methodological work includes the mathematical characterization of the asymptotic distribution of the wavelet estimator (7), as well as further testing of tfBm vs fBm or stationary alternatives.

## 6. REFERENCES

- [1] A. N. Kolmogorov, "The Wiener spiral and some other interesting curves in Hilbert space," *Dokl. Akad. Nauk SSSR*, vol. 26, no. 2, pp. 115–118, 1940.
- [2] S. K. Friedlander and L. Topper, *Turbulence: Classic Papers on Statistical Theory*, Interscience Publishers, 1961.
- [3] A. N. Shiryaev, "Kolmogorov and the turbulence," *University of Aarhus: Centre for Mathematical Physics and Stochastics*, 1999.
- [4] B. Mandelbrot and J. Van Ness, "Fractional Brownian motions, fractional noises and applications," *SIAM Review*, vol. 10, no. 4, pp. 422–437, 1968.
- [5] G. Samorodnitsky and M. Taqqu, *Stable non-Gaussian random processes*, Chapman and Hall, New York, 1994.
- [6] A. Davenport, "The spectrum of horizontal gustiness near the ground in high winds," *Quarterly Journal of the Royal Meteorological Society*, vol. 87, no. 372, pp. 194–211, 1961.
- [7] D. Norton and C. Wolff, "Mobile offshore platform wind loads," in *Offshore Technology Conference*. Offshore Technology Conference, 1981.
- [8] Y. Li and A. Kareem, "ARMA systems in wind engineering," *Probabilistic Engineering Mechanics*, vol. 5, no. 2, pp. 49–59, 1990.
- [9] J.P. Beaupuits, A. Otárola, F. T. Rantakyö, R. C. Rivera, S. J. E. Radford, and LÅ Nyman, "Analysis of wind data gathered at Chajnantor," *ALMA Memo 497, National Radio Astronomy Observatory*, 2004.
- [10] M. Meerschaert and F. Sabzikar, "Tempered fractional Brownian motion," *Statistics & Probability Letters*, vol. 83, no. 10, pp. 2269–2275, 2013.
- [11] M. Meerschaert and F. Sabzikar, "Stochastic integration for tempered fractional Brownian motion," *Stochastic Processes and their Applications*, vol. 124, no. 7, pp. 2363–2387, 2014.
- [12] F. Sabzikar, M. Meerschaert, and J. Chen, "Tempered fractional calculus," *Journal of Computational Physics*, vol. 293, pp. 14–28, 2015.
- [13] L. Giraitis, P. Kokoszka, and R. Leipus, "Stationary ARCH models: dependence structure and central limit theorem," *Econometric Theory*, vol. 16, no. 1, pp. 3–22, 2000.
- [14] Y. Chen, X. Wang, and W. Deng, "Localization and ballistic diffusion for the tempered fractional Brownian-Langevin motion," *Journal of Statistical Physics*, vol. 169, pp. 18–37, 2017.
- [15] M. Meerschaert, F. Sabzikar, M. Phanikumar, and A. Zeleke, "Tempered fractional time series model for turbulence in geophysical flows," *Journal of Statistical Mechanics: Theory and Experiment*, vol. 2014, no. 9, pp. P09023, 2014.
- [16] R. Cont, M. Potters, and J.-P. Bouchaud, "Scaling in stock market data: stable laws and beyond," *Scale Invariance and Beyond*, vol. 7, pp. 75–85, 1997.
- [17] P. Flandrin, "Wavelet analysis and synthesis of fractional Brownian motion," *IEEE Trans. Info. Theory*, vol. 38, no. 2, pp. 910–917, 1992.
- [18] D. Veitch and P. Abry, "A wavelet-based joint estimator of the parameters of long-range dependence," *IEEE Trans. Info. Theory*, vol. 45, no. 3, pp. 878–897, 1999.
- [19] S. Mallat, *A Wavelet Tour of Signal Processing*, Academic Press, San Diego, CA, 1998.
- [20] P. Craigmile, P. Guttorp, and D. Percival, "Wavelet-based parameter estimation for polynomial contaminated fractionally differenced processes," *IEEE Transactions on Signal Processing*, vol. 53, no. 8, pp. 3151–3161, 2005.
- [21] E. Masry, "The wavelet transform of stochastic processes with stationary increments and its application to fractional Brownian motion," *IEEE Transactions on Information Theory*, vol. 39, no. 1, pp. 260–264, 1993.
- [22] J.-M. Bardet, "Statistical study of the wavelet analysis of fractional Brownian motion," *IEEE Transactions on Information Theory*, vol. 48, no. 4, pp. 991–999, 2002.
- [23] V. Anh, C. Heyde, and Q. Tieng, "Stochastic models for fractal processes," *Journal of Statistical Planning and Inference*, vol. 80, no. 1, pp. 123–135, 1999.
- [24] G. Wornell and A. Oppenheim, "Estimation of fractal signals from noisy measurements using wavelets," *IEEE Transactions on Signal Processing*, vol. 40, no. 3, pp. 611–623, 1992.
- [25] E. Moulines, F. Roueff, and M. Taqqu, "A wavelet Whittle estimator of the memory parameter of a nonstationary Gaussian time series," *Annals of Statistics*, pp. 1925–1956, 2008.
- [26] I. Daubechies, *Ten Lectures on Wavelets*, SIAM, 1992.
- [27] A. W. Van der Vaart, *Asymptotic Statistics*, vol. 3, Cambridge University Press, 1998.
- [28] H. Wendt, G. Didier, S. Combexelle, and P. Abry, "Multivariate Hadamard self-similarity: testing fractal connectivity," *Physica D*, vol. 356–357, pp. 1–36, 2017.
- [29] R. Davies and D. Harte, "Tests for Hurst effect," *Biometrika*, vol. 74, no. 1, pp. 95–101, 1987.
- [30] A. Wood and G. Chan, "Simulation of stationary Gaussian processes in  $[0, 1]^d$ ," *Journal of Computational and Graphical Statistics*, vol. 3, no. 4, pp. 409–432, 1994.
- [31] P. Abry, P. Flandrin, M. S. Taqqu, and D. Veitch, "Self-similarity and long-range dependence through the wavelet lens," in *Theory and applications of long-range dependence*, pp. 527–556. Birkhäuser, 2003.
- [32] B. C. Boniece, G. Didier, and F. Sabzikar, "Tempered fractional Brownian motion: wavelet estimation, modeling and testing," *Working paper*, pp. 1–10, 2018.
- [33] W. Palma, *Long-memory Time Series: Theory and Methods*, vol. 662, John Wiley & Sons, 2007.